ELSEVIER

Chemical Engineering Journal 120 (2006) 63–71

Chemical Engineering Journal

www.elsevier.com/locate/cej

Modelling of carbon and hydrogen oxidation kinetics of a coked ferrierite catalyst

T.J. Keskitalo [a,*], K.J.T. Lipiäinen [b], A.O.I. Krause [a]

[a] *Helsinki University of Technology, Department of Chemical Technology, Laboratory of Industrial Chemistry, P.O. Box 6100, FI-02015 TKK, Finland*
[b] *Neste Oil Corporation, Technology Centre, P.O. Box 310, FI-06101 Porvoo, Finland*

Abstract

The hydrocarbons in an alkene skeletal isomerisation process cause catalyst deactivation by forming coke that blocks the active sites. Oxidation of the coke is carried out in a regeneration unit to reactivate the catalyst. A kinetic model for the combustion is essential for purposes of designing the regeneration unit, since the highly exothermic oxidation releases heat that can damage the catalyst and the unit. Kinetic models were derived and tested by non-linear regression against the results of temperature programmed oxidation experiments with a coked ferrierite catalyst. Two methods for the measurement of carbon oxides in the reactor outflow – a direct analysis by mass spectrometry and an indirect analysis by a methanation method – were compared, and both were found appropriate. The determination of water by mass spectrometry was found adequate. The derived models cover the oxidation of both coke carbon and hydrogen. A power law model with an oxygen concentration order of half in carbon oxidation and zero order in hydrogen oxidation described the experimental results well. Two other models, in which active intermediate species are formed in fast equilibrium reactions, performed as well as the power law model. The estimated parameters of the models were in the physically meaningful range.

Keywords: Kinetics; Combustion; Modelling; Catalyst activation; Zeolites; Temperature programmed oxidation (TPO)

1. Introduction

Formation of coke on a catalyst is the main cause of deactivation in skeletal isomerisation of alkenes and in many other catalytic hydrocarbon processes [1]. Skeletal isomerisation of *n*-alkenes is utilised in the production of isoalkenes, which are reactants for fuel components such as *tert*-amyl methyl ether (2-methoxy-2-methylbutane), methyl *tert*-butyl ether (2-methoxy-2-methylpropane), ethyl *tert*-butyl ether (2-ethoxy-2-methylpropane) and isooctane (2,2,4-trimethylpentane). Parts of the hydrocarbons accumulate in the process, forming coke on the catalyst surface and eventually blocking the active sites of the catalyst. Since coke formation is relatively fast, deactivation is essential in an industrial-scale alkene skeletal isomerisation [1,2].

Usually the catalyst is reactivated by oxidation in a regeneration unit. In skeletal isomerisation of alkenes, the coke typically consists of aromatic hydrocarbons, the exact composition of which varies with process parameters [3] such as temperature, the catalyst, feed composition and time-on-stream. The oxidation reactions, in which carbon monoxide, carbon dioxide and water are formed, are highly exothermic. If the combustion is not closely controlled, the generated heat may damage both the catalyst and the regeneration unit. A kinetic model that describes the rates of oxidation reactions is therefore essential for purposes of designing a catalyst reactivation unit.

Temperature programmed oxidation (TPO) is a well-known transient analysis technique [4,5] and a tool applied in many oxidation studies [1]. However, the application of the method is often limited to general properties, such as the main temperature ranges of interest or the total amount of carbon in coke. Through a careful kinetic analysis of the TPO system it is often possible to extract the intrinsic oxidation kinetics as well [1]. The resulting kinetic models can then be applied in the simulation of different reactor set-ups for coke oxidation.

The size of the catalyst particles determines in large measure whether internal diffusion of reactant gases in the particle limits the oxidation rates. If the catalyst particle is small enough, the effect of internal diffusion on observed formation rates of products can be neglected, but otherwise the diffusion must be taken into account in the modelling of any experimental set-up. The studies of Kern and Jess [6] and Tang et al. [7] showed that coke

* Corresponding author. Fax: +358 9 451 2622.
E-mail address: tuomo.keskitalo@tkk.fi (T.J. Keskitalo).

1385-8947/$ – see front matter © 2006 Elsevier B.V. All rights reserved.
doi:10.1016/j.cej.2006.03.033

Nomenclature

$[i]$	concentration of gas phase component i ($\mathrm{mol\,dm^{-3}}$) for $i = O_2$, CO, CO_2 and H_2O, or concentration of intermediate or surface species i ($\mathrm{mol\,g_{cat}^{-1}}$)
E	activation energy ($\mathrm{J\,mol^{-1}}$)
F	molar gas flow rate ($\mathrm{mol\,s^{-1}}$)
ΔH_f	enthalpy of formation ($\mathrm{J\,mol^{-1}}$)
k	reaction rate constant ($\mathrm{s^{-1}}$, $\mathrm{dm^3\,mol^{-1}\,s^{-1}}$ or $\mathrm{g_{cat}\,mol^{-1}\,s^{-1}}$)
K	equilibrium constant ($\mathrm{dm^3\,mol^{-1}}$)
n	amount of moles (mol)
r	reaction rate ($\mathrm{mol\,g_{cat}^{-1}\,s^{-1}}$)
R	molar gas constant ($\mathrm{J\,mol^{-1}\,K^{-1}}$)
t	time (s)
T	temperature (°C)
T_{ref}	reference temperature (K)
x	stoichiometry parameter
v	volumetric flow rate ($\mathrm{dm^3\,s^{-1}}$)
V_g	volume of gas phase ($\mathrm{dm^3}$)
W	mass of catalyst ($\mathrm{g_{cat}}$)

Superscripts

*	intermediate active compound
S	compound adsorbed to surface site

Greek letters

α	reaction order for oxygen concentration
β	reaction order for hydrogen concentration

oxidation rates of Al_2O_3-based catalysts of an industrial particle size (particle diameters 2 and 4.5 mm) are clearly diffusion limited. Tang et al. [7] applied a small particle size (0.05–0.11 mm) to obtain the intrinsic kinetic parameters for combustion.

Quantitative analysis of the reactor outflow must be fast for enough measurements (successive analyses of outflow at different reactor temperatures) to be obtained from a TPO experiment. Measurements must also be accurate even at low concentrations (ppm level). The methanation set-up described by Fung and Querini [8] is a feasible option for the measurement of carbon oxides. In their system, CO and CO_2 are converted into methane, which is detected with a flame ionisation detector. If the output from the TPO reactor is split into two streams and CO_2 is removed from one of them, the CO and CO_2 can be measured separately [9–11]. After carbon oxides in each stream have been quantified, the concentration of CO_2 can be calculated from the difference between the two results. Other detection methods for the analysis of output flow in the TPO set-up [1] include thermal conductivity detection and thermal gravimetric analysis, which do not readily separate CO and CO_2, and mass spectrometry and IR spectrometry, which can be used to detect water in addition to carbon oxides.

Table 1
Enthalpies of formation of gaseous CO, CO_2 and H_2O at 298.15 K [13]

Compound	$\Delta H_{f,298.15\,K}$ ($\mathrm{kJ\,mol^{-1}}$)
CO(g)	−110.50
CO_2(g)	−390.50
H_2O(g)	−241.80

The studies on coke oxidation by TPO often concentrate on carbon oxides, while the evolution of water is not dealt with. However, the combustion of hydrogen contributes to the total heat generation, as indicated by the formation enthalpies of the products of oxidation presented in Table 1, and it should be included when heat generation is considered. Li et al. [10] and Li and Brown [12] attempted to take water, measured with a hygrometer, into account in their modelling of kinetics. They concluded, however, that the adsorption of water on the reactor walls affected the measurements of oxidation rates and their experimental data could not be used in kinetic modelling. Evidently special care must be taken to prevent the adsorption of water on equipment surfaces from interfering with the quantitative analysis in TPO.

The focus of our work is the modelling of coke oxidation kinetics of a ferrierite catalyst deactivated in skeletal isomerisation of alkenes. The experiments were carried out according to the TPO method. Two methods for the quantification of carbon oxides, a direct analysis by mass spectrometry and an indirect methanation method, were compared. The suitability of the measurement of water with a mass spectrometer for kinetic modelling was investigated. In a separate study, we study coke oxidation concentrating on the combustion of carbon alone [14]. This work broadens the approach by including the oxidation of coke hydrogen, and it presents kinetic models that describe the coke oxidation as a whole.

2. Experimental

The experiments for kinetic modelling carried out according to the temperature programmed technique were the same as described elsewhere [14], with the addition of the results from mass spectrometry. The experimental equipment was that described earlier, with an added sampling line from the reactor outlet to the mass spectrometer. Briefly, the equipment consisted of a glass-tube reactor furnished with a small sized Au-film furnace (Neste Oil Corporation), a temperature controller (KS40, Phillips), mass-flow controllers (Brooks), six-way valves (Valco) and the mass spectrometer (Agilent 5973N). The mass fragment m/z 28 was utilised for the detection of CO, m/z 44 for CO_2 and m/z 18 for water. The sampling line to the mass spectrometer was heated to 200 °C and the tube length was minimised to decrease the adsorption of water on the tube walls. Total hydrogen content was measured additionally with a CHN-2000 elemental analyser (LECO).

Kinetic analysis of TPO experiments requires that concentrations of gases in the outflow are analysed quantitatively and that the concentrations are accurately correlated with a reactor temperature. Accordingly pulse experiments with saturated water vapour were carried out to check that the base line was reached

quickly after each pulse. Pulses were produced by introducing helium flow through an autoclave half-filled with water at ambient temperature. Lag time between the TPO reactor and the mass spectrometer was confirmed to be negligible at the applied volumetric flow rate (30 $cm^3\,min^{-1}$, NTP) by routing the water pulse through an empty reactor tube. The pulse experiments were also applied for the calibration of H_2O analysis.

The catalyst was a ferrierite (average particle diameter 120 μm), deactivated in a 21-h skeletal isomerisation run in a pilot-scale reactor operating at 285 °C and 20 kPa [15]. The temperature programmed experimental procedure carried out in situ for each catalyst sample [14] was as follows: a small sample of the coked catalyst (about 10 mg) was maintained at 200 °C for 12 h in helium gas stream to remove adsorbed water. Temperature programmed desorption (TPD) was then carried out at a heating rate of 10 °C min^{-1} up to 500 °C. The sample was maintained at 500 °C until the base output level was reached, and then cooled to 200 °C; after this, TPO (2, 5, 10 or 21 vol.% of O_2 in the feed) was conducted up to 850 °C. Carbon oxides were measured with both methanation equipment [9] and the mass spectrometer, and water was measured with the mass spectrometer. Quantifying of results was based on external calibration, carried out after each TPO step, with calibration gases (CO 0.99 and CO_2 1.99 vol.%, AGA) and water vapour at ambient temperature.

Parameters of several kinetic models were estimated by nonlinear regression to test whether the models describe the results of the oxidation experiments. The object function, which is minimised in the estimation, is the sum of squared residuals over N experimental (exp) and calculated (calc) molar flows of component i out of the reactor:

$$\mathrm{SSR} = \sum_{N,i} \| F_{i,\mathrm{exp}} - F_{i,\mathrm{calc}} \|^2, \quad i = \mathrm{CO}, \mathrm{CO_2}, \mathrm{H_2O} \qquad (1)$$

About 100 measurements of each component for one TPO experiment were applied in modelling. The functions of GNU Scientific Library (GSL) version 1.6 were employed [16]. The Nelder–Mead Simplex and Levenberg–Marquardt optimisation methods were utilised. Where needed, derivatives were evaluated numerically by central differences. The embedded fourth order Runge–Kutta Cash–Karp method of GSL was applied for systems of ordinary differential equations, and the routine RADAU5 [17] was utilised to solve systems of differential-algebraic equations.

3. Results and discussion

3.1. General remarks

Fig. 1 shows the results of a typical TPO experiment. The thermograms were generally smooth and unimodal. The results for water were filtered to better obtain the shape of the curve from noisy experimental data. The CO thermograms generated with the methanation equipment and the mass spectrometer are similar in shape, though a slight difference in scale is observed. The same applies to the CO_2 thermograms. Comparison of the thermograms for water and carbon oxides shows that water output continues after the output of carbon oxides has ceased. This

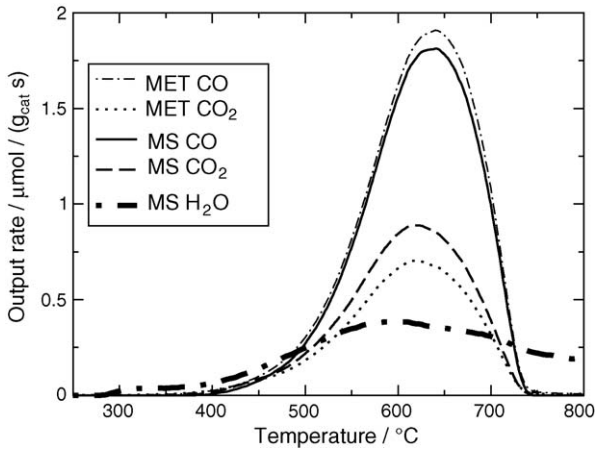

Fig. 1. Results of a TPO experiment with the coked catalyst, analysed with methanation equipment (MET) and a mass spectrometer (MS), carried out at a heating rate of 10 °C min^{-1} with 2 vol.% of O_2 in feed.

is counterintuitive if the water originates from coke oxidation. Since coke is composed of hydrocarbons, one would in that case expect the release of water to cease at the same or a lower temperature than the release of carbon oxides.

The evolved water does not originate from the coke oxidation alone. The results of an experiment following the procedure described above but carried out with a fresh catalyst sample (Fig. 2) show a release of water starting from 500 °C. A possible explanation of this is that the structure of the ferrierite begins to break up, and water is released from the crystal lattice of the zeolite [1]. This explanation is favoured by the fact that the catalyst has been calcined at 550 °C, a temperature close to the start of water generation from the fresh sample. Another possibility is that the thermogram results from adsorbed water of an origin different from coke oxidation.

The water thermograms applied in modelling were derived by subtracting the results obtained with the fresh catalyst from those obtained with the coked ones (described below). Since heating rate affects the thermogram, two experiments at each heating rate (5, 10 and 15 °C min^{-1}) were carried out with the

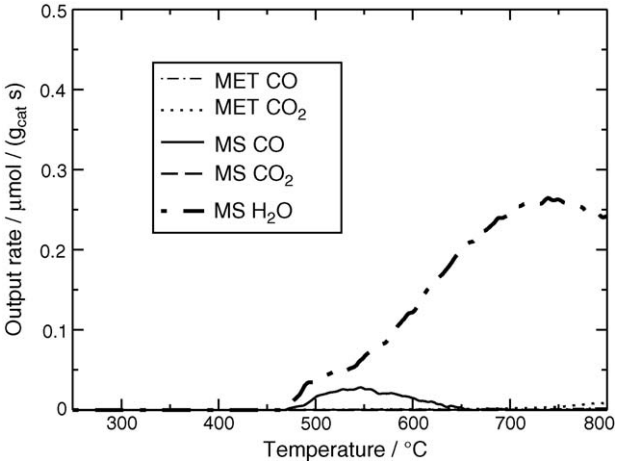

Fig. 2. Results of an experiment with a fresh catalyst, carried out at a heating rate of 10 °C min^{-1} with 2 vol.% of O_2 in feed. MET denotes the methanation equipment and MS the mass spectrometer.

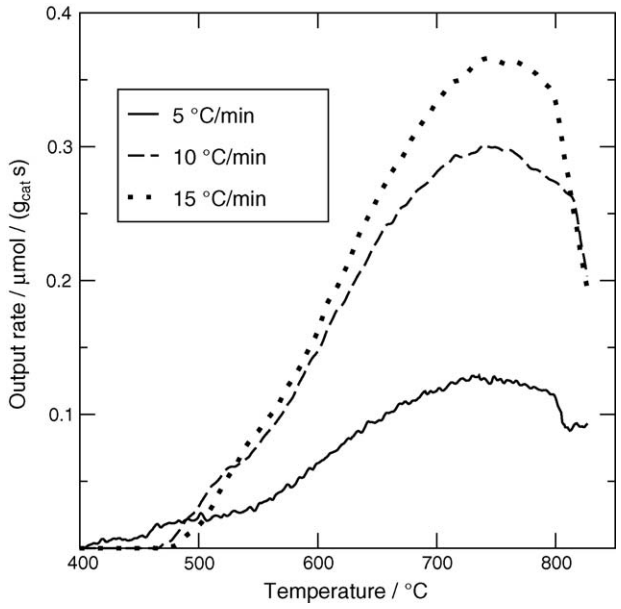

Fig. 3. Average water thermograms from fresh catalyst at the heating rates of 5, 10 and 15 °C min^{-1}.

fresh catalyst. The average of the two experiments conducted at the particular heating rate was applied for each thermogram of the coked sample. The average thermograms are presented in Fig. 3. We assume that the data obtained by the preprocessing of the experimental data described above represent the water originating from coke oxidation and the data are thus applicable in the kinetic modelling.

Fig. 4 depicts the total amounts of CO, CO_2 and H_2O assumed to originate from coke oxidation and evolved in 23 TPO experiments. The total amounts do not show any significant trend as a function of either the heating rate or oxygen concentration. As already noted, the shapes of the CO and CO_2 thermograms are closely similar, so either method of analysis could be used in modelling. The average total amount of carbon originating from coke oxidation in TPO experiments measured with the methanation equipment (2.75 ± 0.19 mmol g_{cat}^{-1}) is very close to that obtained with the mass spectrometer (2.73 ± 0.33 mmol g_{cat}^{-1}). Another measure, the ratio of the total evolved amounts of CO to CO_2 obtained with the methanation equipment is slightly higher (2.14 ± 0.33) than the corresponding ratio obtained with the mass spectrometer (1.88 ± 0.37). The two values are nevertheless close to each other.

Since the results obtained with the methanation equipment exhibited smaller standard deviation of the total amounts, we chose to utilise them in modelling. The results of the three experiments carried out at the heating rate of 10 °C min^{-1} and oxygen concentration 2 vol.% were used to calculate cross-validation errors (CVE) for the models. All other experimental data were applied in the estimation of parameters.

The average total amount of water assumed to originate from coke oxidation in the TPO experiments was 0.71 ± 0.26 mmol g_{cat}^{-1} (0.14 ± 0.05 wt.%). The total hydrogen content 0.4 wt.%, measured with the LECO elemental analyser, was higher than the calculated value, as expected, because part of the hydrogen in the coke is removed during the TPD step

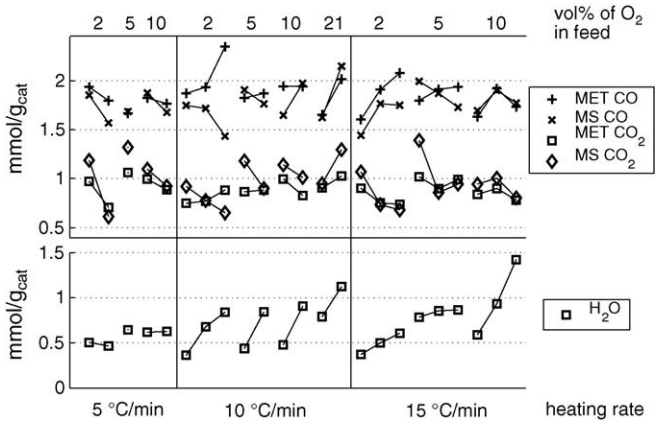

Fig. 4. Total amounts of CO, CO_2 and H_2O originating from coke oxidation in TPO experiments.

carried out prior to TPO. The molar ratio of carbon to hydrogen in the coked catalyst sample, calculated from the LECO results, is about 1.0. The ratio prior to TPO calculated from the amounts of water and carbon oxides assumed to originate from coke oxidation is about 1.9, so the coke loses more hydrogen than carbon during the TPD step, and the coke becomes more aromatic.

Fig. 5 depicts thermograms of oxides assumed to originate from coke oxidation in selected TPO experiments. The release of water ceased before or simultaneously with the release of carbon oxides, which is the behaviour expected for coke oxidation. In a few experiments at the heating rate of 15 °C min^{-1}, evolution of water ceased as much as 100 °C higher than the evolution of carbon oxides. However, even this value is in the range of experimental errors related to setting of the baseline and the preprocessing of the experimental data for water described above.

Fig. 5 shows that the evolution of water originating from coke oxidation consistently begins earlier than the evolution of carbon oxides, and it ends slightly before or at the same temperature as for the carbon oxides. Evidently hydrogen is oxidised more easily than carbon. Li and Brown [12] made the same observation. The overlapping of the thermograms may be the result of some sort of interdependence of carbon and hydrogen combustion. Since the coke is composed of both species, it is even likely that the oxidations of carbon and hydrogen are interdependent at some level.

3.2. Modelling

The microreactor was modelled as a gradientless reactor, since calculations showed that the space time of the reactor is small in relation to the observed reaction rates, no significant concentration or heat gradients are present in the reactor, and internal diffusion is not a limiting factor [14]. The molar balance of oxygen was omitted too, because calculations indicated that the reactions did not markedly affect the oxygen concentration in the reactor gas phase. The mass balances for the molar

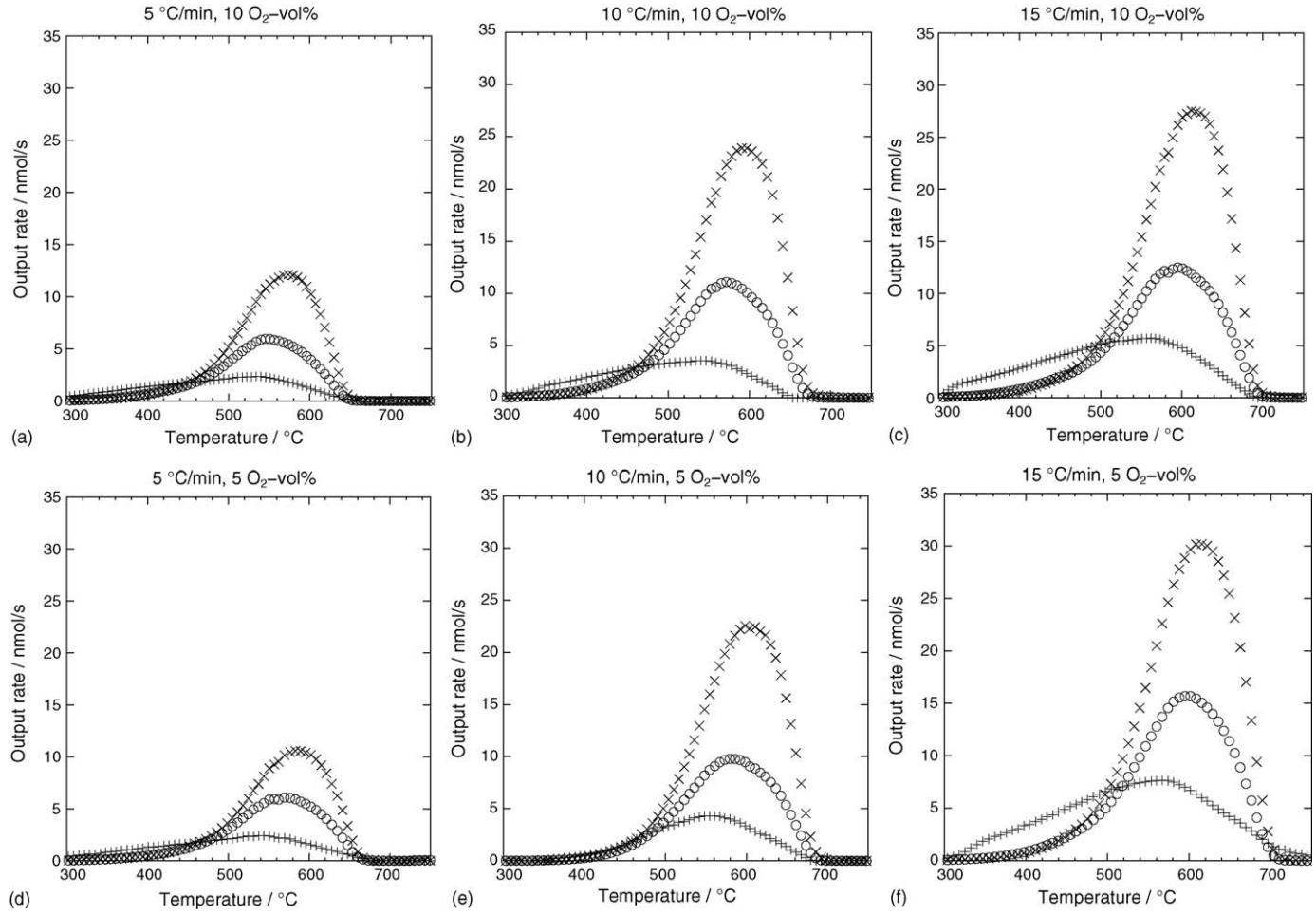

Fig. 5. Results of selected TPO experiments. The thermograms are assumed to represent oxides from coke oxidation. CO response is denoted with the symbol (×), CO_2 with (O) and H_2O with (+).

amounts of oxides in the reactor gas phase are

$$\frac{dn_i}{dt} = r_i W - \frac{v n_i}{V_g}, \quad i = \mathrm{CO}, \mathrm{CO_2}\ \text{or}\ \mathrm{H_2O} \tag{2}$$

The second term at the right side of Eq. (2) represents the flow out of the reactor and it is related to Eq. (1) by

$$F_{i,\mathrm{calc}} = \frac{v n_i}{V_g} \tag{3}$$

The kinetic models presented in the following aim at describing the rates of overall oxidation reactions of the carbon (C) and the hydrogen (H) in the coke:

$$\mathrm{C} + \tfrac{1}{2}\mathrm{O_2(g)} \rightarrow \mathrm{CO(g)} \tag{4}$$

$$\mathrm{C} + \mathrm{O_2(g)} \rightarrow \mathrm{CO_2(g)} \tag{5}$$

$$2\mathrm{H} + \tfrac{1}{2}\mathrm{O_2(g)} \rightarrow \mathrm{H_2O(g)} \tag{6}$$

The concentrations of carbon and hydrogen prior to TPO (initial values of the calculation for each experiment) were calculated by integration of the experimental thermograms of the oxides. By default, all the estimated reaction rate constants are dependent on temperature by the reparametrised Arrhenius equation:

$$k_i = k_{\mathrm{ref},i}\, \mathrm{e}^{(-E_i/R)(1/T - 1/T_{\mathrm{ref}})} \tag{7}$$

The reference temperature was 850 K. Mass balances for each component were calculated by summing over all the reaction rates of the steps relevant to the component. Correlation coefficients of the parameter pairs with absolute value larger than 0.95 are reported.

We first concentrate on the oxidation of hydrogen. Model 1 for reaction (6) is

$$r_1 = k_1[H] \tag{8}$$

The order of hydrogen concentration in the model is unity, and this model described the experiments relatively well (residual root mean square (RRMS) value 0.31 nmol s^{-1}). The estimated values for the parameters are $k_{\mathrm{ref},1} = (1.22 \pm 0.09) \times 10^{-3}\ s^{-1}$ and $E_1 = 50 \pm 3\ \mathrm{kJ\ mol^{-1}}$. A more complex power law model:

$$r_{1\mathrm{b}} = k_{1\mathrm{b}}[\mathrm{O_2}]^{\alpha_{1\mathrm{b}}}[H]^{\beta_{1\mathrm{b}}} \tag{9}$$

was tested as well, but the order of hydrogen concentration approached a value near unity ($\beta_{1\mathrm{b}} = 1.05 \pm 0.03$) and the order of oxygen concentration approached zero, and the model fit (RRMS value 0.30 nmol s^{-1}) was almost the same as with rate

Table 2
Estimated parameter values and corresponding 95% confidence intervals, residual root mean square values and cross-validation errors for model 2

Parameter	Value
$k_{\mathrm{ref,2a}}$	$(1.22 \pm 0.09) \times 10^{-3}\ \mathrm{s}^{-1}$
E_{2a}	$50 \pm 3\ \mathrm{kJ\ mol}^{-1}$
$k_{\mathrm{ref,2b}}$	$(6.6 \pm 0.5) \times 10^{-2}\ \mathrm{dm}^3\ \mathrm{mol}^{-1}\ \mathrm{s}^{-1}$
E_{2b}	$127 \pm 2\ \mathrm{kJ\ mol}^{-1}$
α_{2b}	0.59 ± 0.02
$k_{\mathrm{ref,2c}}$	$(1.7 \pm 0.3) \times 10^{-2}\ \mathrm{dm}^3\ \mathrm{mol}^{-1}\ \mathrm{s}^{-1}$
E_{2c}	$99 \pm 3\ \mathrm{kJ\ mol}^{-1}$
α_{2c}	0.50 ± 0.03
RRMS value	$0.90\ \mathrm{nmol\ s}^{-1}$
CVE value	$0.91\ \mathrm{nmol\ s}^{-1}$

The parameters for reactions (11) and (12) (subscripts 2b and 2c) are the same as reported in [14].

expression (8). Rate expression (9) essentially reduced to (8). In another test, the hydrogen reaction order was fixed to 2.0, but the model fit deteriorated (RRMS value $0.47\ \mathrm{nmol\ s}^{-1}$), which indicates that the order of hydrogen oxidation in reaction (5) is probably not two.

The effectively zero order of oxygen concentration indicates that the oxygen concentration in the tested range (2–21 vol.%) does not markedly affect the oxidation rate of hydrogen. In contrast to the oxidation of hydrogen, an oxygen concentration order of about 0.5 was found to be best for the oxidation of carbon [14]. Clearly, the overall oxidations of carbon and hydrogen differ with respect to order of oxygen concentration.

Model 2 is a combination of separate power law models for hydrogen oxidation (model 1) and carbon oxidation [14]:

$$2\mathrm{H} \overset{+\mathrm{O_2(g)}}{\rightarrow} \mathrm{H_2O(g)}, \quad r_{2a} = k_{2a}[\mathrm{H}] \tag{10}$$

$$\mathrm{C} \overset{+\mathrm{O_2(g)}}{\rightarrow} \mathrm{CO(g)}, \quad r_{2b} = k_{2b}[\mathrm{C}][\mathrm{O_2}]^{\alpha_{2b}} \tag{11}$$

$$\mathrm{C} \overset{+\mathrm{O_2(g)}}{\rightarrow} \mathrm{CO_2(g)}, \quad r_{2c} = k_{2c}[\mathrm{C}][\mathrm{O_2}]^{\alpha_{2c}} \tag{12}$$

The model describes the experimental results well (RRMS value $0.90\ \mathrm{nmol\ s}^{-1}$) and is used as a reference later on. The parameters of model 2 are given in Table 2. The correlations between the parameter pairs $k_{\mathrm{ref,2b}}$, α_{2b} and $k_{\mathrm{ref,2c}}$, α_{2c} were high (absolute value of correlation coefficient larger than 0.95), but they did not prevent convergence to a unique optimum. Several different initial values for the parameters were tested to check that the optimum was reached.

As already stated, the oxidations of hydrogen and carbon may be interdependent. Models 3 and 4 were derived to test for a form of dependence. The dependence is included in the models through a hydrocarbon species, which contains both carbon and hydrogen (CH_x^*). Model 3 describes the oxidation of a carbon species (C) and (CH_x^*), and model 4 describes the oxidation of a hydrogen species (H) and (CH_x^*).

Model 3 is described by

$$\tfrac{2}{x}\mathrm{CH}_x^* \overset{+\mathrm{O_2(g)}}{\rightarrow} \tfrac{2}{x}\mathrm{C} + \mathrm{H_2O}, \quad r_{3a} = k_{3a}[\mathrm{CH}_x^*][\mathrm{O_2}]^{\alpha_{3a}} \tag{13}$$

$$\mathrm{C} \overset{+\mathrm{O_2(g)}}{\rightarrow} \mathrm{CO}, \quad r_{3b} = k_{3b}[\mathrm{C}][\mathrm{O_2}]^{\alpha_{3b}} \tag{14}$$

$$\mathrm{C} \overset{+\mathrm{O_2(g)}}{\rightarrow} \mathrm{CO_2}, \quad r_{3c} = k_{3c}[\mathrm{C}][\mathrm{O_2}]^{\alpha_{3c}} \tag{15}$$

The model includes a stoichiometry parameter x, which defines the atomic ratio of hydrogen to carbon in the species CH_x^*. Reaction rate expressions (13)–(15) include the order of oxygen concentration as a parameter. The molar amounts of C and CH_x^* prior to TPO (initial state in the calculation) for each experiment were determined from the total amounts of carbon and hydrogen (obtained by integration of the experimental thermograms) and the stoichiometry parameter x so that all hydrogen was incorporated in the species CH_x^*, and all carbon not in the species CH_x^* was contained in C. The molar amounts were converted into concentrations by normalising with the catalyst mass.

The value of x increased to values larger than 50 during optimisation. Several initial values were tested to confirm this result. A high value of x corresponds to very low amount of carbon in the species CH_x^*, and the model is thus reduced to separate power law models for hydrogen and carbon oxidation (model 2). The model fit (RRMS value $0.90\ \mathrm{nmol\ s}^{-1}$) was equal to that of model 2, and the parameters were very close to those of model 2.

Model 4 includes the following oxidation steps and rates:

$$2\mathrm{H} \overset{+\mathrm{O_2(g)}}{\rightarrow} \mathrm{H_2O}, \quad r_{4a} = k_{4a}[\mathrm{H}][\mathrm{O_2}]^{\alpha_{4a}} \tag{16}$$

$$\mathrm{CH}_x^* \overset{+\mathrm{O_2(g)}}{\rightarrow} \mathrm{CO} + xH, \quad r_{4b} = k_{4b}[\mathrm{CH}_x^*][\mathrm{O_2}]^{\alpha_{4b}} \tag{17}$$

$$\mathrm{CH}_x^* \overset{+\mathrm{O_2(g)}}{\rightarrow} \mathrm{CO_2} + xH, \quad r_{4c} = k_{4c}[\mathrm{CH}_x^*][\mathrm{O_2}]^{\alpha_{4c}} \tag{18}$$

The concentration of H and CH_x^* prior to TPO were calculated similarly to C and CH_x^* in model 3, but in this case all carbon was included in CH_x^* and some of the hydrogen was available as the pure hydrogen species H. The optimized value of the stoichiometry parameter x was 0.022 ± 0.014, which indicates that very little hydrogen is present in the hydrocarbon species. As before, the model was reduced to model 2 (RRMS value $0.90\ \mathrm{nmol\ s}^{-1}$) and the parameters were near to those of model 2.

Models 3 and 4 can be interpreted as including an inhibition effect for oxidation. In model 3 the carbon included in the species CH_x^* is not available for the oxidation reactions (14) and (15) until released by reaction (13). The same applies for hydrogen in model 4. However, this kind of dependence of carbon and hydrogen oxidation is not supported by the results of models 3 and 4: both the models were essentially reduced to a non-dependent power law model (model 2).

One possible explanation for the failure of models 3 and 4 is that they incorrectly describe the dependence of carbon and hydrogen oxidation. It is also possible that the available experimental data is not informative enough for the dependence to be extracted by modelling. All experiments were carried out with the same deactivated catalyst, which has the same concentrations of carbon and hydrogen prior to TPO. Variation in concentrations would provide more information about the dependence.

As suggested by the results with models 3 and 4, the overall oxidations of carbon and hydrogen may be essentially independent, or dependent through species other than coke carbon and

Table 3
Estimated parameter values and corresponding 95% confidence intervals, residual root mean square values and cross-validation errors for model 5

Parameter	Value
K_{5a}	$(7.6 \pm 0.1) \times 10^2$ dm^3 mol^{-1}
$k_{ref,5b}$	$(2.74 \pm 0.02) \times 10^{-3}$ s^{-1}
E_{5b}	125 ± 1 kJ mol^{-1}
$k_{ref,5c}$	$(1.34 \pm 0.01) \times 10^{-3}$ s^{-1}
E_{5c}	102 ± 1 kJ mol^{-1}
$k_{ref,5d}$	$(2.43 \pm 0.05) \times 10^{-3}$ s^{-1}
E_{5d}	50 ± 1 kJ mol^{-1}
RRMS value	0.80 nmol s^{-1}
CVE value	0.71 nmol s^{-1}

Table 4
Estimated parameter values and corresponding 95% confidence intervals, residual root mean square values and cross-validation errors for model 6

Parameter	Value
K_{6a}	$(7.35 \pm 0.01) \times 10^2$ dm^3 mol^{-1}
K_{6b}	2.9×10^{-2} dm^3 mol^{-1} [a]
$k_{ref,6c}$	3.8 g_{cat} mol^{-1} s^{-1} [a]
E_{6c}	118 ± 1 kJ mol^{-1}
$k_{ref,6d}$	1.0×10^2 s^{-1} [a]
E_{6d}	250 ± 110 kJ mol^{-1}
$k_{ref,6e}$	4.9×10^1 s^{-1} [a]
E_{6e}	230 ± 110 kJ mol^{-1}
$k_{ref,6f}$	7.4×10^2 g_{cat} mol^{-1} s^{-1} [a]
E_{6f}	50 ± 2 kJ mol^{-1}
$[S_0]$	1.1 mmol g_{cat}^{-1} [a]
RRMS value	0.80 nmol s^{-1}
CVE value	0.65 nmol s^{-1}

[a] Large confidence interval.

hydrogen. Models 5 and 6 describe this last possibility. The models are extensions of the ones reported in [14].

Model 5 includes one intermediate species on the catalyst or coke surface (CO_2^*). The oxidation proceeds according to reactions:

$$C + O_2(g) \leftrightharpoons CO_2^*, \quad K_{5a} = \frac{[CO_2^*]}{[C][O_2]} \tag{19}$$

$$CO_2^* \rightarrow CO(g) + O^\bullet, \quad r_{5b} = k_{5b}[CO_2^*] \tag{20}$$

$$CO_2^* \rightarrow CO_2(g), \quad r_{5c} = k_{5c}[CO_2^*] \tag{21}$$

$$H_2(s) \rightarrow H_2^*, \quad r_{5d} = k_{5d}[H_2] \tag{22}$$

$$H_2^* + CO_2^* \rightarrow C + H_2O(g) + O^\bullet, \quad r_{5e} = r_{5d} \tag{23}$$

In reaction (19), carbon forms an intermediate species CO_2^* in a fast equilibrium reaction with oxygen. Carbon oxides are formed from the intermediate species in reactions (20) and (21). Coke hydrogen is assumed to be a solid dihydrogen species ($H_2(s)$). An active dihydrogen (H_2^*) is formed from the dihydrogen in reaction (22). The active dihydrogen is then oxidised by CO_2^* and forms water by reaction (23). The rate of reaction (23) is assumed to be fast relative to reaction (22), which makes reaction (22) the rate limiting step in hydrogen oxidation, and therefore the rate of reaction (22) is applied in (23). The species $O^\bullet$ is included only to balance the stoichiometry of the reactions and has no other importance in the reaction scheme. Combination of $O^\bullet$ to gas phase dioxygen may occur, for example. The model fit was good (RRMS value 0.80 nmol s^{-1}).

Model 5 exhibits no strong correlations between parameters, and its parameter estimates (Table 3) are reliable and in the physically meaningful range. The activation energies of model 5 (E_{5b}, E_{5c} and E_{5d}, corresponding to the reaction steps of CO, CO_2 and H_2O formation, respectively) are close to those in model 2 (E_{2b}, E_{2c} and E_{2a}), which underlines the similarity of the models. The values of the rate coefficients are clearly different, and thus the kinetics of the reaction steps differ from each other. The values of the activation energies also show that the oxidation of hydrogen requires less energy than the oxidation of carbon, and the formation of CO requires more energy than the formation of CO_2.

Selected experimental and simulated model 5 thermograms are shown in Fig. 6. All other models that fit well gave closely similar TPO responses. The model output for the evolution of water assumed to originate from coke oxidation does not closely match the experimental one, but the fit is considered adequate. The applied preprocessing of the experimental water data necessarily reduces the precision of the data, and more detailed models for hydrogen oxidation with the available experimental data would probably result in overfitting.

According to model 6, oxygen adsorbs both associatively and dissociatively on a site on the catalyst surface (S):

$$O_2(g) + S \leftrightharpoons O_2^S, \quad K_{6a} = \frac{[O_2^S]}{[O_2][S]} \tag{24}$$

$$O_2(g) + 2S \leftrightharpoons 2O^S, \quad K_{6b} = \frac{[O^S]^2}{[O_2][S]^2} \tag{25}$$

The associatively adsorbed oxygen (O_2^S) reacts further with carbon by

$$C + O_2^S \rightarrow CO_2^S, \quad r_{6c} = k_{6c}[C][O_2^S] \tag{26}$$

$$CO_2^S \rightarrow CO(g) + O^S, \quad r_{6d} = k_{6d}[CO_2^S] \tag{27}$$

$$CO_2^S \rightarrow CO_2(g) + S, \quad r_{6e} = k_{6e}[CO_2^S] \tag{28}$$

and the dissociatively adsorbed oxygen (O^S) reacts with coke dihydrogen species ($H_2(s)$) by

$$H_2(s) + O^S \rightarrow H_2O(g) + S, \quad r_{6f} = k_{6f}[H_2][O^S] \tag{29}$$

According to this model, the associatively adsorbed oxygen contributes to the oxidation of carbon, while the dissociatively adsorbed oxygen contributes to the oxidation of hydrogen. The estimated parameters of model 6 are presented in Table 4. Correlations were high for the parameter pair $k_{ref,6c}$, [S0] and for the group of parameters $k_{ref,6d}$, $k_{ref,6e}$, E_{6d} and E_{6e}, resulting in unreliable estimates for many parameters. Although the parameter estimates of model 6 were not reliable, the model fits the experimental data as well as model 5 (RRMS value 0.80 nmol s^{-1}). The model may thus be an appropriate description of the rate limiting steps of coke oxidation.

Even though the actual elementary reactions of combustion are numerous [18], the relatively simple models presented in this paper describe the overall coke combustion well enough for

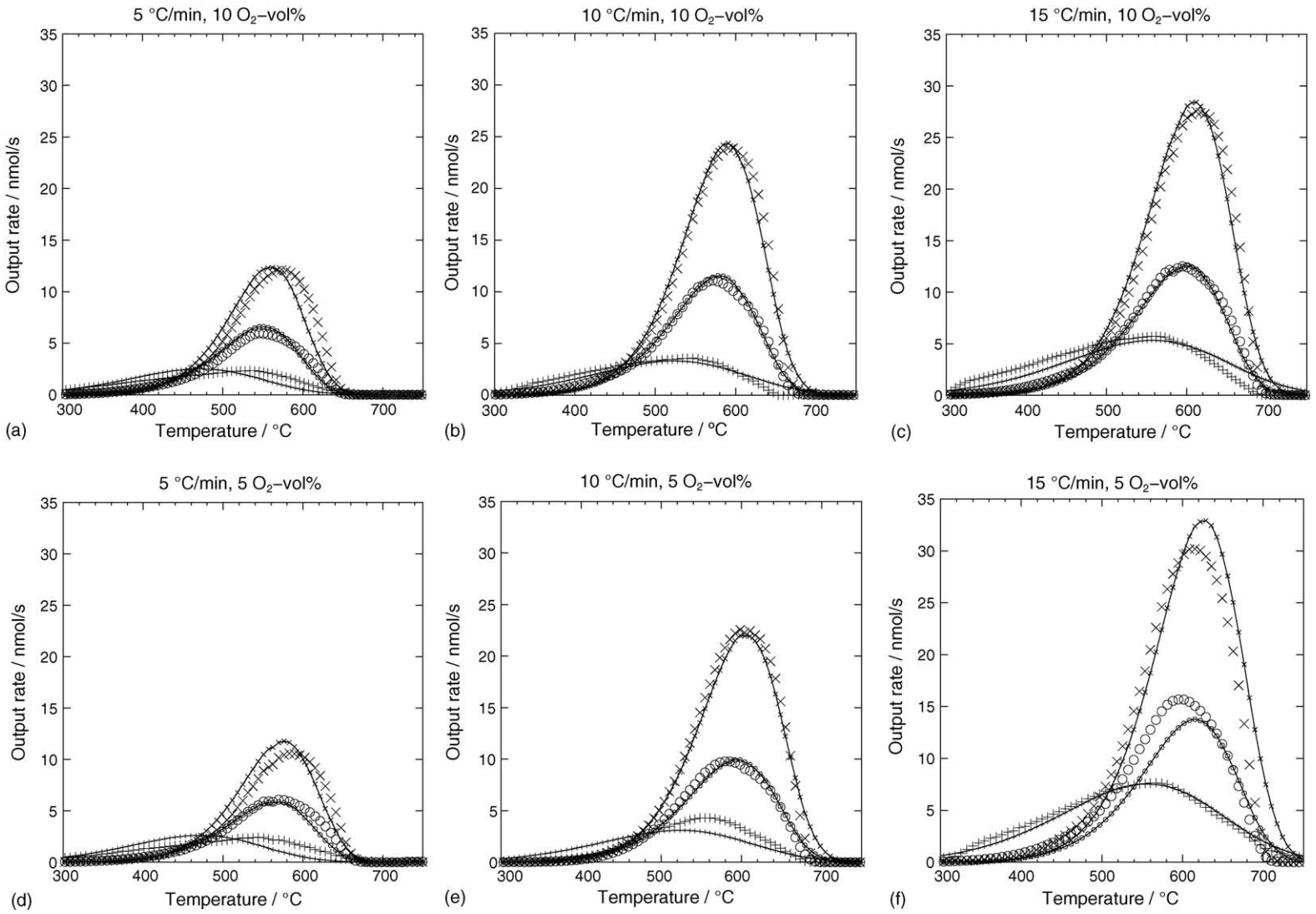

Fig. 6. Experimental (large symbols) and model 5 simulation (continuous lines, small symbols) results of selected TPO experiments. CO response is denoted with symbol (×), CO_2 with (O) and H_2O with (+).

engineering purposes. Models 2, 5 and 6 all describe the results of oxidation experiments, but only the parameter estimates of models 5 and 2 are well-identified. The cross-validation errors of models 6 and 5 are similar (0.65 and 0.71 nmol s^{-1}, respectively), while model 2 performs slightly worse in this respect (0.91 nmol s^{-1}). Models 5 and 2 appear to be the best kinetic models for purposes of designing a regeneration unit.

4. Conclusions

Results of temperature programmed oxidation experiments were utilised for modelling of coke oxidation kinetics. Two methods for the quantitative analysis of carbon oxides – a direct analysis with a mass spectrometer and an indirect methanation set-up – were compared. Both methods were found suitable for TPO. The quality of the analysis of water with the mass spectrometer was confirmed to be adequate. The water evolved from the ferrierite catalyst originated in coke oxidation and other sources, which were distinguished by subtracting the averaged water thermograms of experiments with a fresh catalyst from those with the coked one.

Kinetic analysis of the experimental data led to the identification of reliable models for the oxidation of coke carbon and hydrogen. These models can be applied in the design of a catalyst regeneration unit. A power law model that combined the independent oxidations of carbon and hydrogen described the experimental results well. Two other models, in which active intermediate oxygen species are formed in fast equilibrium reactions and which include a dependence of carbon and hydrogen oxidation through these intermediate species, described the experimental results as well as the power law model.

Acknowledgements

Neste Oil Corporation and the National Technology Agency of Finland funded the work. The authors thank Tuija Stenbäck for carrying out the experiments.

References

[1] C.A. Querini, Catalysis 17 (2004) 166–209.
[2] P. Meriaudeau, C. Naccache, Adv. Catal. 44 (2000) 505–543.
[3] S. van Donk, J.H. Bitter, K.P. de Jong, Appl. Catal., A 212 (2001) 97–116.
[4] J.A. Schwarz, J.L. Falconer, Catal. Today 7 (1990) 1–92.
[5] S. Bhatia, J. Beltramini, D.D. Do, Catal. Today 7 (1990) 309–438.
[6] C. Kern, A. Jess, Chem. Eng. Sci. 60 (2005) 4249–4264.
[7] D. Tang, C. Kern, A. Jess, Appl. Catal., A 272 (2004) 187–199.
[8] S.C. Fung, C.A. Querini, J. Catal. 138 (1992) 240–254.
[9] K. Lipiäinen, P. Hagelberg, J. Aittamaa, I. Eilos, J. Hiltunen, V.-M. Niemi, A.O.I. Krause, Appl. Catal., A 183 (1999) 411–421.
[10] C. Li, C.L. Minh, T.C. Brown, J. Catal. 178 (1998) 275–283.
[11] C.L. Minh, R.A. Jones, I.E. Craven, T.C. Brown, Energy Fuels 11 (1997) 463–469.
[12] C. Li, T.C. Brown, Energy Fuels 13 (1999) 888–894.
[13] C.L. Yaws, Chemical Properties Handbook, McGraw-Hill, 1999.
[14] T.J. Keskitalo, K.J.T. Lipiäinen, A.O.I. Krause, manuscript in preparation.
[15] F. Sandelin, I. Eilos, E. Harlin, J. Hiltunen, J. Jakkula, J. Makkonen, M. Tiitta, in: E. van Steen (Ed.), Proceedings of the 14th International Zeol. Conference, (2004) 2157–2162.
[16] M. Galassi, J. Davies, J. Theiler, B. Gough, G. Jungman, M. Booth, F. Rossi, GNU Scientific Library Reference Manual, 2nd ed., Network Theory Limited, United Kingdom, 2003.
[17] E. Hairer, G. Wanner, Solving Ordinary Differential Equations. Part II. Stiff and Differential-Algebraic Problems, Springer, Berlin, Germany, 1996.
[18] J.A. Miller, M.J. Pilling, J. Troe, Proc. Comb. Inst. 30 (2005) 43–88.